Electronic Supplementary Material (ESI) for Chemical Communications.

Electrochemiluminescence Platform for Transcription Factor Diagnosis by Using CRISPR-Cas12a Trans-Cleavage Activity

Zhenqiang Fan,[a] Yuedi Ding,[a] Bo Yao,[a,b] Jiaying Wang,*[,c] Kai Zhang,*[,a]

[a] *NHC Key Laboratory of Nuclear Medicine, Jiangsu Key Laboratory of Molecular Nuclear Medicine, Jiangsu Institute of Nuclear Medicine, Wuxi, Jiangsu, China.*

[b] *Key Laboratory of Flexible Electronics (KLOFE) & Institute of Advanced Materials (IAM), Jiangsu National Synergetic Innovation Center for Advanced Materials (SICAM), Nanjing Tech University (NanjingTech), 30 South Puzhu Road, Nanjing 211816, P.R. China.*

[c] *Drug Clinical Trial Institution, Nanjing Medical University, Affiliated Wuxi People's Hospital, Wuxi, Jiangsu 214000, China.*

* Corresponding author. Fax: +86-510-85508775; Tel: +86-510-85508775

E-mail addresses: jiayingwang@njmu.edu.cn (J. Wang), zhangkai@jsinm.org (K. Zhang)

1. Experimental section

1.1 Materials and chemicals

Relevant oligonucleotides synthesized and purified through the polyacrylamide gel electrophoresis (PAGE) method during the whole experiments for the fabrication of the ECL biosensor and the assays process were purchased from Genscript Biotechnology Co., Ltd (Nanjing, China). The specific sequences involved are listed in Table S1. N-(3-(Dimethylamino)propyl)-N-ethyl-carbodiimide hydrochloride (EDC), N-hydroxysuccinimide (NHS), triethylamine and other analytical grade chemicals reagents, were obtained from Aladdin Biochemical Technology Co. Ltd. (Shanghai, China). Tris (4,4'-dicarboxylic acid-2,2'-bipyridyl) ruthenium (II) dicbloride ($Ru(dcbpy)_3^{2+}$) was purchased from Suna Tech Inc. (Suzhou, China). Au nanocages and polyethyleneimine (PEI) modified graphene oxide nanosheets (GO-PEI) were purchased from XFNANO (Nanjing, China). NF-κB p50 (human recombinant) was got from Hengfei Biotechnology Co. Ltd. (Shanghai). Tris(2-carboxyethyl) phosphine hydrochloride (TCEP) and tris-borate-EDTA (TBE) buffer were from Sangon Biotech Co. Ltd. (Shanghai). Phosphate buffered saline (PBS, pH = 7.1) buffer was acquired from Beyotime Biotechnology Co. Ltd. (Shanghai). The ultrapure water needed for the experimental process was treated by the Milli-Q purification system (Branstead) and maintained a resistance of 18.2 MΩ.

1.2 Instruments and measurements

Electrochemical impedance spectroscopy (EIS) and cyclic voltammetry (CV) measurements were performed with CHI 660E (Chenhua Apparatus Co., Ltd, Shanghai). The parameters of EIS experiments carried in 0.1 M PBS solution (pH = 7.4) containing 5 mM $[Fe(CN)_6]^{3-/4-}$ are set as follows: 5 mV amplitude and 0.1 to 10 kHz frequency. During the ECL assays for NF-κB p50 detection, a three-electrode system consisting of a working (glassy carbon) electrode (GCE), a reference (Ag/AgCl) electrode, and a counter (platinum) electrode was provided by the State Key Laboratory of Analytical Chemistry for Life Science, Nanjing University. Transmission electron

microscopy (TEM) images were got by 1400 PLUS (Japanese electronics). Atomic force microscope (AFM) images were obtained by Dimension ICON (Bruker).

1.3 Synthesis of RuGO-Au

RuGO-Au was prepared regarding a previous study and slightly modified as follows [1]. First, 10 mg of $Ru(dcbpy)_3^{2+}$ was dissolved into 5 mL of water to obtain 2 mg mL^{-1} of the ECL emitter solution. Then, 2.5 mL of EDC (7 mg mL^{-1}) solution was added to the ECL aqueous solution to activate the -COOH of $Ru(dcbpy)_3^{2+}$ for 15 min. After that, 2.5 mL of NHS aqueous solution (2 mg mL^{-1}) was added and stirred continuously for 2 h to obtain the pre-activated solution. Finally, 10 mL of Au nanoparticles with a diameter of about 13 nm were added to the above mixture and kept stirring for 3 h. Based on the electrostatic interaction of the Au-N bond, a stable solution of the ECL emitter complex solution was obtained. The mixture solution was then centrifuged to remove excess chemicals, and then the synthesized RuGO-Au material was diluted into 5 mL of pure water for further modification.

1.4 Preparation of DTs and Au nanocage modified S3 probe

The DTs was synthesized with a 71-nucleotide DNA strand (T1) and three 59-nucleotide thiolated DNA strands (T2, T3 and T4) as follows: First, T2, T3, and T4 were incubated in PBS containing 10 mM TCEP for 40 min at room temperature for pretreatment. Then, the mixture of T1, T2, T3, and T4 with the final concentrations (1 μM) was shaken slightly and mixed well. Next, the mixture was heated to 95 °C and incubated for 15 min, and then cooled to 4 °C to get the programmable DTs with high purity and stability. The synthesis of DTs was then verified by non-denaturing polyacrylamide gel electrophoresis (PAGE, 15%). Experiments were run in TBE (89 mM Tris-bolic-acid, 2 mM EDTA, pH = 7.4) buffer at 115 V for 2.5 h at room temperature. Afterward, it was stained with ethidium bromide (EB) for 20 min and then imaged by UV light (ChemiDoc MP, Bio-Rad). For further use, the successfully synthesized DTs was stored in a refrigerator (4 °C).

The Au nanocage modified S3 probes (2 μM) were prepared using the following surfactant-assisted

method: 20 μL of 1 wt % Tween 20 and 40 μL of mPEG-SH (10 μM) with a molecular weight of 5 kDa were added to 2 mL of Au nanocage (2 nM). After a slight oscillation for ten minutes, 20 μL of TCEP-treated S3 (100 μM) was added to the above mixture overnight. Then, 0.3 mL of PBS solution containing 4 M NaCl was added to incubate for 1 h for stabilizing the modified probes. Finally, the mixture was centrifuged, washed twice with PBS and redispersed into 1 mL of PBS for storage in a refrigerator at 4 °C.

1.5 ECL Biosensor preparation

First of all, GCE cleaning preparation was performed prior to ECL biosensor preparation to get a spotless electrode. First, the GCE with a diameter of 3 mm was soaked in a piranha solution consisting of 98% H_2SO_4 and 30% H_2O_2 (ratio 4:1) to remove non-specific adsorbed materials attached to the GCE. Then, the GCE was polished with 0.05-μm-sized alumina powder and repeatedly sonicated in water and ethanol solution to obtain clean, mirror-like GCE to finish the cleaning preparation. Subsequently, the clean GCE was activated in H_2SO_4 (0.1 M) solution and continuously scanned at a sweep rate of 0.1 V s^{-1} in the potential range of –0.8–0.8 V. The activation of the electrode is completed when a stable CV characteristic peak is obtained. After rinsing with pure water, the electrode was dried under a dry N_2 atmosphere and was ready for the following modification of the ECl emitter complex as well as the nucleic acid probes.

Secondly, 8 μL of RuGO-Au solution was dripped onto the cleaned GCE surface and subsequently dried under nitrogen to obtain RuGO-Au/GCE. After that, the modified electrode was immersed into DTs solution and incubated overnight to obtain DTs/RuGO-Au/GCE by forming Au-S covalent bonds. Then, the modified electrode was immersed into the 100 μL Au nanocage modified S3 DNA (2 μM) solution for 2 h to obtain Au-S3/DTs/RuGO-Au/GCE, here, acting as an ECL biosensor for NF-κB p50 detection.

1.6 Quantification Assay

DNA1 and DNA2 with the same concentration of 20 μM were hybridized in buffer 1 (50 mM Tris-

HCl, 100 mM NaCl, and 1 mM EDTA), by heating to 90 °C for 5 min and cooling to 4 °C for 2 h to form stable DNA duplexes. Then, 20 μL of specific concentrations of NF-κB p50 were incubated with DNA duplexes in buffer 2 (10 mM Tris-HCl, 100 mM KCl, 2 mM $MgCl_2$, 0.1 mM EDTA, 10% glycerol, and 0.25 mM DTT) for 45 min at room temperature.

Next, the above protein-binding solution was added to buffer 3 (20 mM Tris-HCl, 100 mM KCl, 5 mM $MgCl_2$, 5% glycerol and 1 mM DTT) containing 100 nM CRISPR-Cas12a/gRNA. Subsequently, the ECL biosensor Au-S3/DTs/RuGO-Au/GCE was immersed in the reaction solution for 1 h. After the incubation, the biosensor was rinsed with PBS twice. The ECL signals were then collected in 0.1 M PBS (pH = 7.4) containing 18 mM co-reactant TEA with the potential scan ranged from 0 to 1.3 V.

2. Results and discussion

2.1 Characterization of DTs

To verify the successful assembly of the ECL biosensor, we first validated the fabrication of DTs scaffold probe. PAGE was used to demonstrate its synthesis, as shown in Fig. S1A. As the four ssDNA gradually assembled from T1 to T4, it could see that the stripe speed was progressively slower, which was consistent with the expected assembly of DNA tetrahedra, indicating the successful synthesis of the DTs. Then we characterized the morphology and particle size of DTs, as shown in Fig. 2B. The AFM two-dimensional (2D) morphology image visually depicted that the synthesized DTs had a regular size and were uniformly distributed on the freshly cleaved mica. We randomly selected four points (a, b, c, and d) in Fig. S1B and their height profiles were shown in Fig. S1C. The height profiles indicated the heights of DTs particles were ranged from 5.91 to 7.27 nm. Based on the fact that the average height of each base was 0.34 nm, we calculated the height of our programmed DTs to be 4.72 nm and the length of each prong to be 5.73 nm. Therefore, the measured DTs height was slightly higher than the theoretical value, which was attributed to the effect of capture DNA at the vertices of the tetrahedron prongs on the practically measured height. We also selected more points in the 2D AFM image to statistically characterize the height, as shown

in Fig. S1D. The median and mean values were 6.96 nm and 6.86 nm, respectively, yielding a statistical height of 6.86±0.56 nm, which was also in line with expectations, indicating that the tetrahedral probe scaffold was successfully prepared and could be further used for the construction of ECL biosensor.

2.2 Characterization of quencher probes

The Au nanocage in our strategy was to absorb the energy emitted by the RuGO-Au emitter. The TEM image (Fig. S2A) showed that the Au nanocage was a hollow and porous nanoparticle with a diameter of about 40 nm. In addition, the dynamic light scattering (DLS) data (Fig. S2B) also showed that the diameter of the Au nanocage with narrow distribution was approximately 39 nm, which was corresponding to the visualized size in Fig. S2A. We also compared the UV-vis spectra of the Au nanocage with that modified with S3 DNA probe (Fig. S2C). The spectra showed the characteristic peak of Au nanocage was 655 nm and the appearance of the characteristic absorption peaks of the DNA probe (S3) at 260 nm for S3-Au nanocage indicated that S3 probe was successfully modified to Au nanocage. We also compared the Zeta potential of S3-Au nanocage with Au nanocage (Fig. S2D), where S3-Au nanocage possessed more negative charges, which confirmed the successful binding of the S3 DNA probe to Au nanocage.

2.3 Comparison of DNA tetrahedron-based and ssDNA-based interfaces

Our constructed DNA tetrahedral interface compared to the conventional ssDNA-based constructed sensors in terms of improved hybridization efficiency, improved sensor sensitivity and specificity to distinguish target from non-specific proteins. First, we verified the hybridization efficiency of DNA tetrahedra and ssDNA with S3-Au nanocage, respectively, illustrated by the quenching efficiency (I_E) of the signals (Fig. S3A). The results show that the quenching efficiency of DNA tetrahedra and ssDNA probes for the sensing interface is 53.47% and 12.25%, respectively, which indicates that DNA tetrahedra can improve the hybridization efficiency for capture probes compared with conventional ssDNA. We also validated the sensing ability of DNA tetrahedron-based versus ssDNA sensors at different target protein concentrations (Fig. S3B). We found that the ECL signal

of the ssDNA-based sensor did not change with increasing concentration until the target concentration reached 1 pM. However, the LOD of the DNA tetrahedron-based sensor is 10.9 fM, which is much lower than the detection capability of the ssDNA-based sensor, suggesting that our DNA tetrahedron can significantly enhance the sensitivity of the sensor. We also compared the ECL performance of the ssDNA-based sensor with that of the DNA tetrahedron-based sensor at the same target concentration of 10 pM as shown in Fig. S3C. The S/N value reflects the intensity of the signal, and a value close to 1 indicates a weak signal response, which is close to the blank sample, so that it is not easily distinguished from other non-specific proteins. The S/N values of 0.647 and 0.958 for the DNA tetrahedron-based and ssDNA-based sensors, respectively, indicate that the DNA tetrahedron-based sensing platform exhibits a stronger ability to differentiate between targets and non-specific proteins at the same target concentration.

2.4 Specificity and stability validation of the ECL biosensor

We explored the specificity of the CRISPR-Cas12a-based ECL biosensor, both for other non-specific proteins and gRNA-like mutation sites. In our experiments on other non-specific proteins (as depicted in Fig. S4A), the other non-specific proteins showed nearly the same ECL intensity as the blank sample, which was much higher than the ECL intensity of the NF-κB p50, indicating that our ECL detection strategy was highly specific for the target protein. Three gRNAs (gRNA1, gRNA2 and gRNA3) with mutated sites, whose specific base sequences were shown in Table S1, were also compared with gRNA (as depicted in Fig. S4B). In the experiments on gRNA specificity, only gRNA was replaced by other gRNAs with mutated bases (gRNA1, gRNA2 and gRNA3), and other test conditions were kept constant. We observed that the ECL intensity of gRNAs with mutated bases only slightly stronger ECL intensity than the blank sample, which was significantly lower than the ECL signal of gRNA as the crRNA sequence, due to the stronger recognition of gRNA with the DNA1/DNA2 duplex and the presence of the mutated site resulted in the inability to activate the cleavage activity of CRISPR-Cas12a. We also investigated the stability of the assay system (as depicted in Fig. S4C) by probing the ECL signal values for 10 cycles at 100 fM and 100 pM, and the calculated relative standard deviation (RSD) was 1.92% and 1.17%, respectively, which were both in the range of less than 5%, indicating the good stability of our assay system.

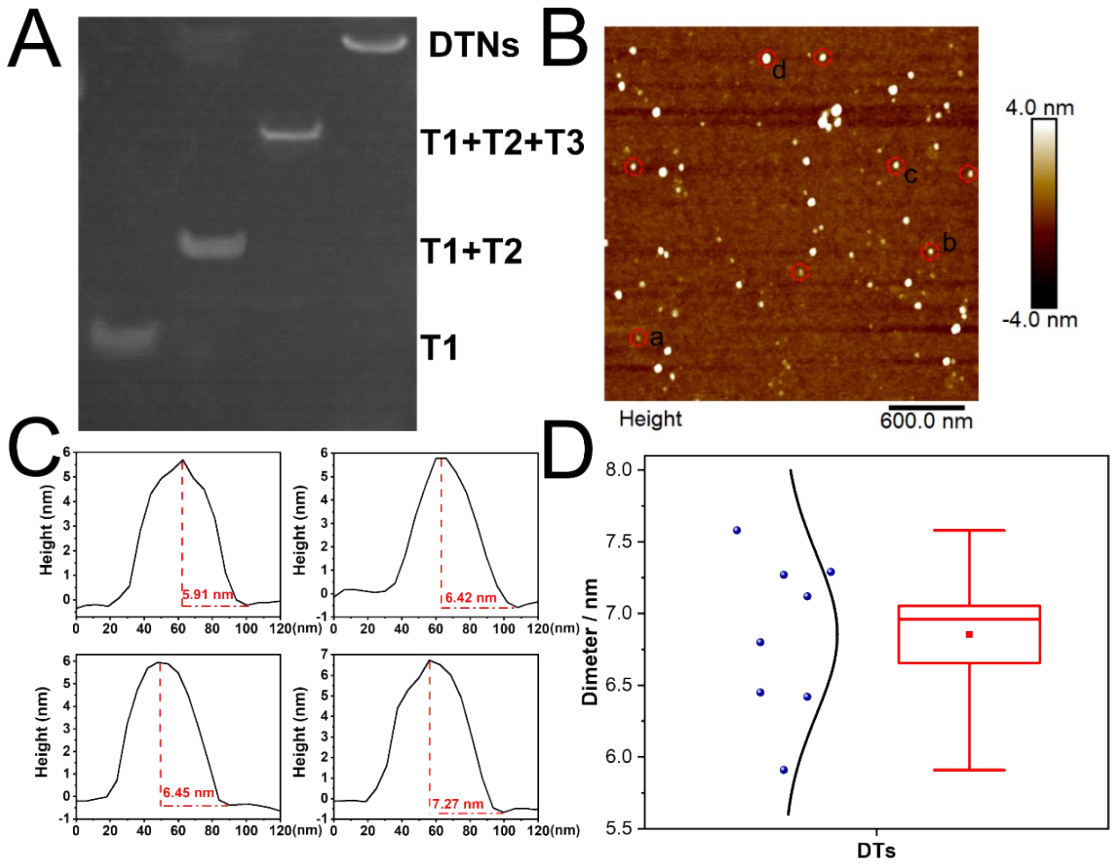

Fig. S1 (A) PAGE image for illustrating the formation of the DTs, (B) 2D AFM image of DTs on freshly cleaved mica. (C) Practical heights of the DTs marked with a, b, c, d in Fig. 2B. (D) Box chart for showing the height distribution of the points marked with circles in Fig. 2B. The actual heights of the DTs counted were presented by the column scatter plots. The curve nearby was showing the normal distribution situation. The square point of the box was the mean value and the parallel line on the upper side was the median value.

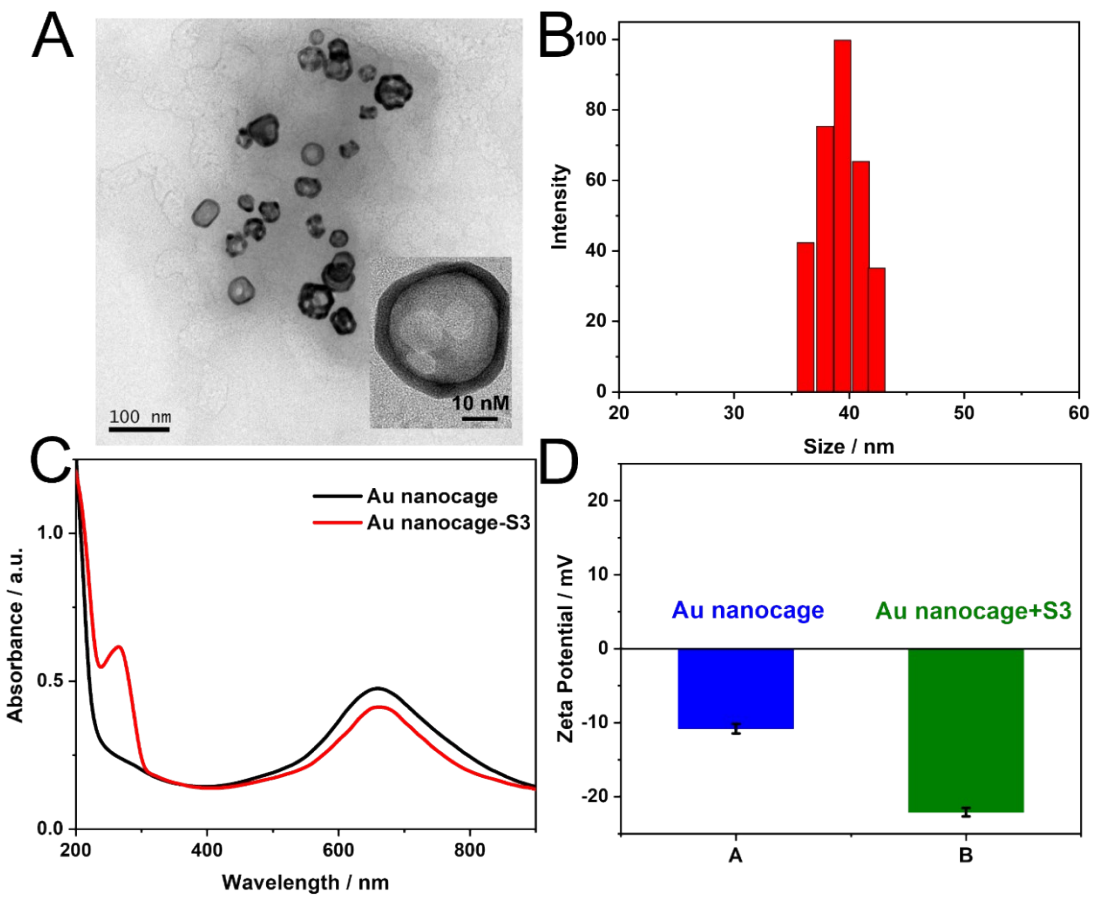

Fig. S2 (A) TEM image of Au nanocages with 100 nm scale bar, the inset was the magnified TEM image with 10 nm scale bar. (B) DLS characterization of the Au nanocages. (C) UV-vis spectra of Au nanocage and S3 modified Au nanocage. (D) Zeta potentials of Au nanocage and S3 modified Au nanocage.

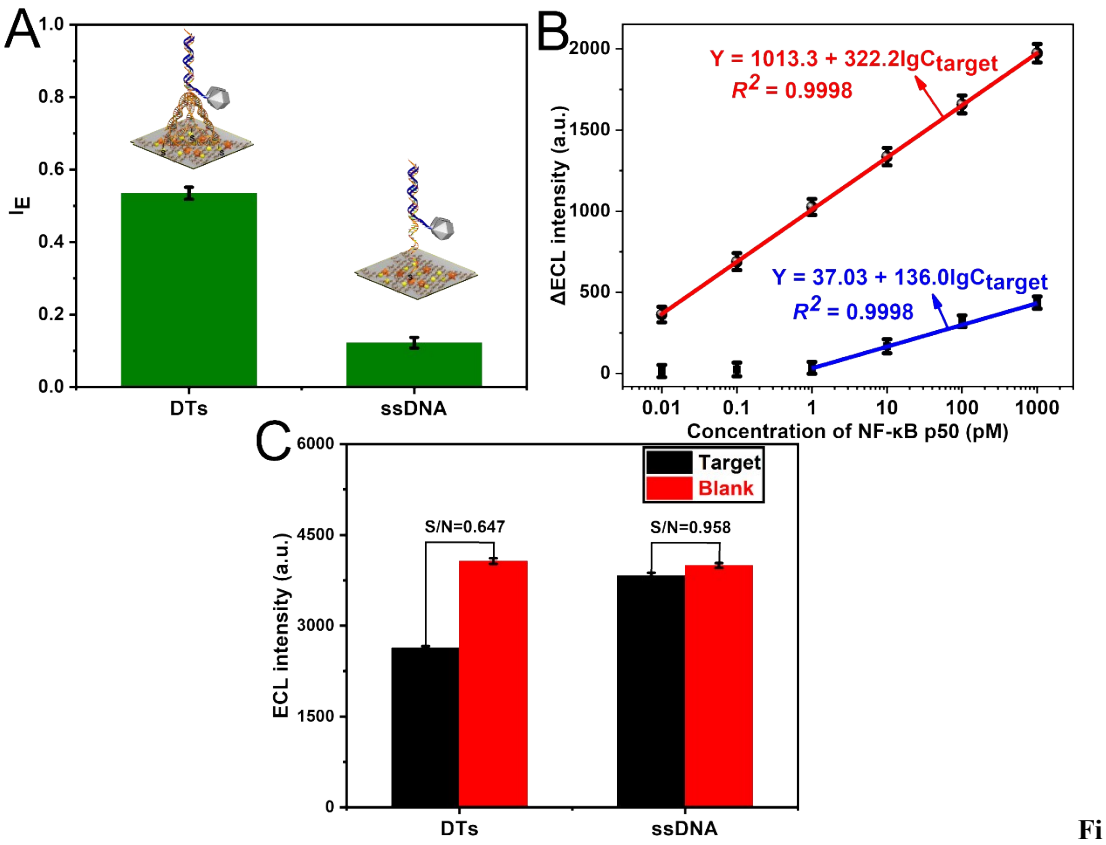

Fig. S3 (A) The comparison of ECL quenching efficiency based on DNA tetrahedra versus ssDNA probes, respectively. (B) Relationship between the values of ECL intensity changes and logarithmic NF-κB p50 concentration values based on DNA tetrahedra (upper curve) and ssDNA (lower curve). (C) Performance comparison of DNA tetrahedron-based and ssDNA-based sensors (10 pM of target protein).

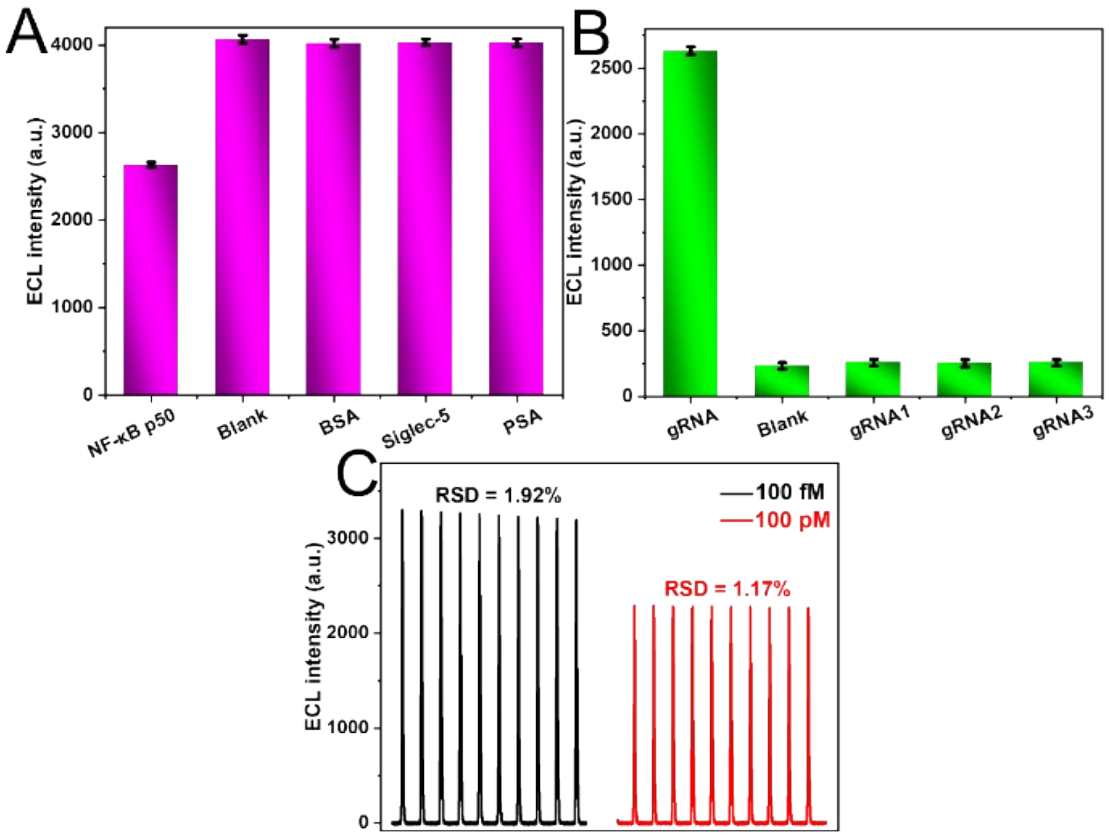

Fig. S4 Specificity and stability validation of the ECL biosensor for NF-κB p50 detection based on CRISPR-cas12a cleavage characteristics: (A) ECL intensity of target protein and three non-specific proteins (BSA, Siglec-5 and PSA) and (B) ECL intensity of gRNA analogs containing different mutation sites. (The specificity experiments based on target proteins as well as specific gRNAs were performed with other variables held constant); (C) Stability validation of the sensor at different NF-κB p50 concentrations (100 fM and 100 pM).

Table S1. Oligonucleotides sequences involved in the experiments. The underlined sequences of DNA1 and DNA2 are the specific binding sequences for NF-κB p50.

note	sequence (5'-3')
T1	TGC TTT CTT CAA CTT AGA ACT CTT ACT TAA ACC TTG ATA CTC ACG ATC ATC CTT TTC TCT TGG CTG CTT GT
T2	HS-TTT TAG AGC CCT ATA TGT TTG TTC GTT CTA TTA GGT GAT ATT GGT TTA AGT AAG AGT TC
T3	HS- TTT TCA CCA CCT CCC TCA AGA TTT ATC ACC TAA TAG AAC GTT ACA AGC AGC CAA GAG AA
T4	HS- TTT TTC TTG AGG GAG GTG GTG TTG GAT GAT CGT GAG TAT CTA CAA ACA TAT AGG GCT CT
S3	HS- TTTTTTTTTT TAA GTT GAA GAA AGC A
gRNA	UAAUUUCUACUCUUGUAGAU G GAA AGU CCC GUA UAA GUG AA
gRNA1	UAAUUUCUACUCUUGUAGAU G GAA AAU CCC GUA UAA GUG AA
gRNA2	UAAUUUCUACUCUUGUAGAU G GAA AAU UCC GUA UAA GUA AA
gRNA3	UAAUUUCUACUCUUGUAGAU U GAA AGU CCA GUA UAA GUU AA
DNA1(TS)	TCA CTT ATA C<u>GGG ACT TTC C</u> TAAA CCCAAA CGC ATA
DNA2(NTS)	TAT GCG TTTGGG TTTA <u>G GAA AGT CCC</u> GT ATA AGT GA

Table S2. Comparisons of sensitivity and limit of detection (LOD) with other transcription factor detecting methods reported previously.

Method	Linear range	LOD	Ref.
Fluorescence	0 to 200 pM	0.5 pM	2
Fluorescence	30 pM to 1.5 nM	10 pM	3
Fluorescence	10 to 50 pM	0.54 pM	4
ECL	0 to 300 pM	3.2 pM	5
ECL	10 pM to 10 nM	5.8 pM	6
ECL	50 pM to 2 nM	17 pM	7
Colorimetric	5 to 2000 pM	3.8 pM	8
Colorimetric	0 to 120 nM	10 nM	9
ECL	10 fM to 1 nM	10.9 fM	This work

REFERENCES

1. J. Ye, L. Zhu, M. Yan, Q. Zhu, Q. Lu, J. Huang, H. Cui and X. Yang, *Anal. Chem.*, 2019, **91**, 1524-1531.
2. K. Zhang, K. Wang, X. Zhu and M. Xie, *Chem. Commun.*, 2017, **53**, 5846-5849.
3. B. Li, L. Xu, Y. Chen, W. Zhu, X. Shen, C. Zhu, J. Luo, X. Li, J. Hong and X. Zhou, *Anal. Chem.*, 2017, **89**, 7316-7323.
4. J. Li, J. Tang, B. Jiang, Y. Xiang and R. Yuan, *J. Mater. Chem. B*, 2018, **6**, 6002-6007.
5. Z. Fan, J. Wang, N. Hao, Y. Li, Y. Yin, Z. Wang, Y. Ding, J. Zhao, K. Zhang and W. Huang, *Chem. Commun.*, 2019, **55**, 11892-11895.
6. Z. Fan, Z. Lin, Z. Wang, J. Wang, M. Xie, J. Zhao, K. Zhang and W. Huang, *ACS Appl. Mater. Interfaces*, 2020, **12**, 11409-11418.
7. Y. Xiong, L. Lin, X. Zhang and G. Wang, *RSC Advances*, 2016, **6**, 37681-37688.
8. Y. Zhang, J. Hu and C.-y. Zhang, *Anal. Chem.*, 2012, **84**, 9544-9549.
9. L.-J. Ou, P.-Y. Jin, X. Chu, J.-H. Jiang and R.-Q. Yu, *Anal. Chem.*, 2010, **82**, 6015-6024.